Int. J. Multiphase Flow Vol. 11, No. 6, pp. 783–796, 1985
Printed in Great Britain.

0301-9322/85 $3.00 + .00
Pergamon/Elsevier

INFLUENCE OF NONUNIFORM PARTICLE SIZE ON SETTLING BENEATH DOWNWARD-FACING INCLINED WALLS

UWE SCHAFLINGER
Institut für Strömungslehre and Wärmeübertragung, Technische Universität Wien, Vienna, Austria

(*Received* 21 *September* 1984; *in revised form* 28 *February* 1985)

Abstract—Experimental observations of the settling process in a symmetrical, roof-shaped vessel show a deformation of the initially horizontal interface between the suspension and the clear fluid, if Re^2/Gr is small and Re^4/Gr is large. This phenomenon is the result of a particle stream moving upward with a relatively high velocity within a sub-boundary-layer between the bulk of the suspension and a clear liquid layer that is formed underneath the inclined walls of the vessel. This particle stream propagates into the clear liquid above the suspension, thus giving rise to the observed deformities with the shape of protruding "horns" and, as a consequence, to an oscillation of the interface. A possible reason for these effects could be the nonuniform particle size. This assumption is confirmed by a theoretical analysis, which proves the existence of the abovementioned sub-boundary layer for the special case of two different particle sizes.

1. INTRODUCTION

Several models have already been suggested in order to provide theoretical predictions of the sedimentation in vessels with inclined walls. Hill *et al.* (1977) found numerical solutions of the two-phase-flow equations for a very dilute suspension of particles. The settling of a dilute suspension in a narrow channel between two parallel plates was studied experimentally and theoretically by Herbolzheimer & Acrivos (1981) and Leung & Probstein (1983). Settling in vessels whose aspect ratio is of order unity has been investigated by Acrivos & Herbolzheimer (1979) and Schneider (1982). A theory for the time-dependent settling of a dilute suspension in a rotating conical channel was quite recently given by Amberg *et al.* (1984). Anestis & Schneider (1983) presented an application of the theory of kinematic waves to the centrifugation of suspensions.

On using dimensional analysis the process of settling is described by two dimensionless groups: Re, a sedimentation Reynolds number, and Gr, a sedimentation Grashof number, which are defined as follows:

$$\mathrm{Re} = HU/\nu_f, \qquad [1]$$

$$\mathrm{Gr} = H^3 g\alpha_0(\rho_s - \rho_f)/\rho_f\nu_f^2, \qquad [2]$$

where H is a characteristic height of the suspension, α_0 the initial volume fraction of the solid phase, g the gravitational constant, ρ the density and ν the kinematic viscosity. The subscript f refers to the clear fluid, and the subscript s to the solids. U is the settling velocity of an individual particle and given, for instance by Stokes' law

$$U = \frac{d^2(\rho_s - \rho_f)g}{18\rho_f\nu_f}, \qquad [3]$$

where d is the diameter of the spheres.

The analysis by Acrivos & Herbolzheimer (1979) requires both Re^2/Gr and Re^4/Gr to be small. These authors showed that the settling rate can be predicted from the well-known PNK formula due to Ponder (1925) and Nakamura & Kuroda (1937). This is incorrect, however, when centered waves appear within the suspension in the case of a certain range of α_0 (Schneider 1982). Apart from this fact, the deviations from the PNK formula reported in

the literature (Zahavi & Rubin 1975; Kinosita 1949) are probably due to flow instabilities (Herbolzheimer 1983) and nonuniform particle size in the suspension.

In the present paper the latter case will be the subject of investigations in order to find an explanation for experimentally observed effects (Schaflinger 1985) such as "horns" and resuspending particles (figure 1). The analysis will be an extension of the theory by Schneider (1982), which is valid for small values of Re^2/Gr and large values of Re^4/Gr and leads to a two- or three-dimensional kinematic wave theory for the bulk flow. The analysis of Schneider allows a subsequent calculation of the clear liquid boundary layer, where in a first approximation the flow is inviscid and quasi-steady. Our calculations are mainly concerned with the influence of nonuniform particle size on the behaviour of the boundary layer underneath inclined walls. As shown later, the structure of the particle sub-boundary-layer depends on Gr/Re^3. Only the limiting case of $Gr/Re^3 \to 0$ gives rise to an inviscid sublayer. Aside from the abovementioned investigations, Schneider *et al.* (1985) investigated the sediment composition due to settling of particles of different sizes. Smith (1966) studied the sedimentation of particles having a dispersion of sizes in vessels with vertical walls. He showed that the volume fraction of the slower particles in the upper region differs from its initial value and can be calculated from continuity of the flux across the interface. Davis *et al.* (1982) derived solutions for settling rates and concentration distributions within the

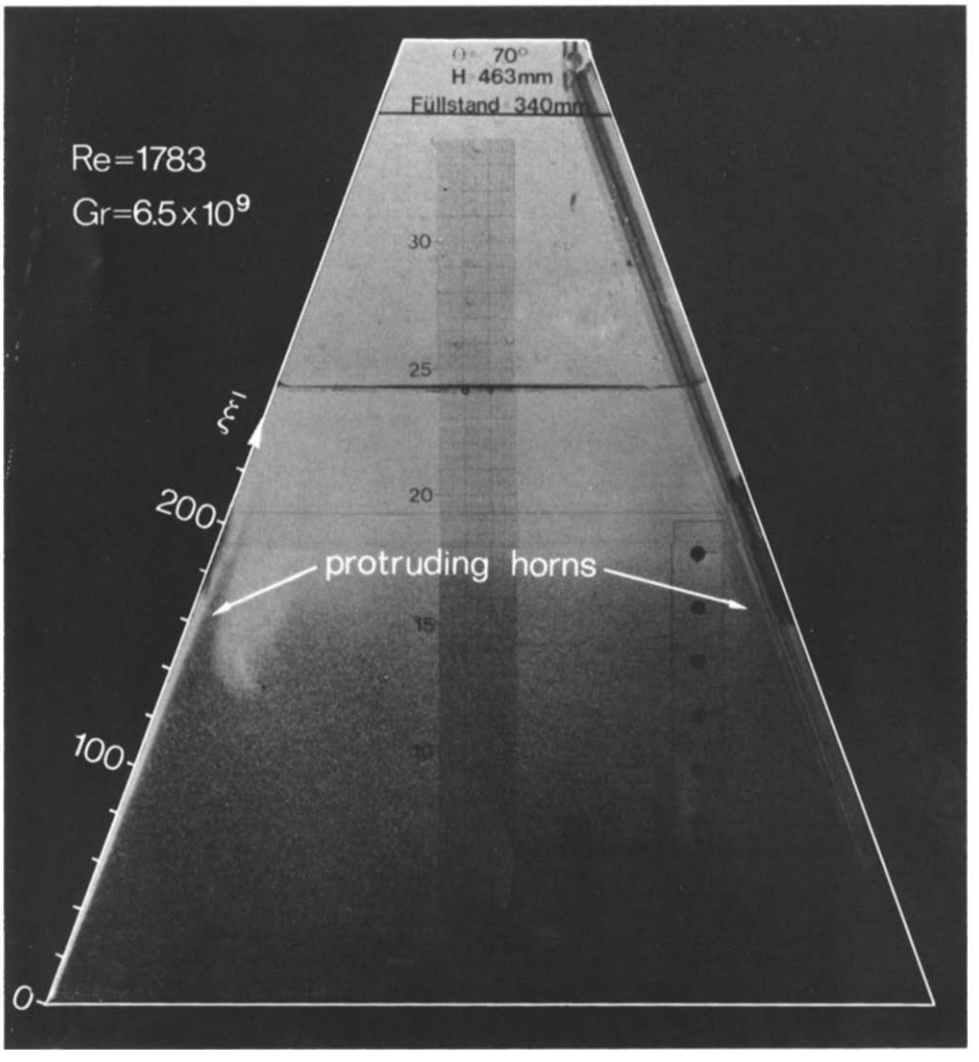

Figure 1. Observation of the flow.

suspension during sedimentation of polydispersed suspensions in vessels having inclined walls but did not consider the influence on the boundary layer. Greenspan & Ungarish (1982) studied a hindered settling of particles of different sizes and determined volume fractions and distributions, as well as the composition of the sedimentary layer.

2. BASIC EQUATIONS AND PREVIOUS RESULTS

We introduce dimensionless variables by referring all volume flux densities and velocities to U, all lengths to H, the height of the vessel, and the time t to H/U (figure 2). In section 3 and the following sections U is replaced by U_A.

With the total volume flux density $\mathbf{j} = \mathbf{j}_f + \mathbf{j}_s$, the equations of continuity for the solid phase and the mixture are, respectively,

$$\frac{\partial \alpha}{\partial t} + \nabla \mathbf{j}_s = 0, \qquad [4]$$

$$\nabla \mathbf{j} = 0. \qquad [5]$$

In applications of batch sedimentation both Gr/Re and Gr/Re^2 are usually very large. Therefore, the momentum equation of the mixture is reduced to

$$\nabla \bar{P} = \alpha \left(\frac{\rho_s}{\rho_f} - 1 \right) \mathbf{e}. \qquad [6]$$

where $\mathbf{e}$ is the unit vector in direction of gravity and P is a dimensionless pressure according to $\nabla P = (\nabla P - \mathbf{g}\rho_f)/g\rho_f$.

According to the arguments due to Schneider (1982), it may be shown by applying the curl operator to [6] that the partial particle concentration of each particle species in a polydispersed suspension has to be constant within the bulk in any horizontal plane at any instant of time.

The momentum equation of the relative motion is reduced to a functional relation

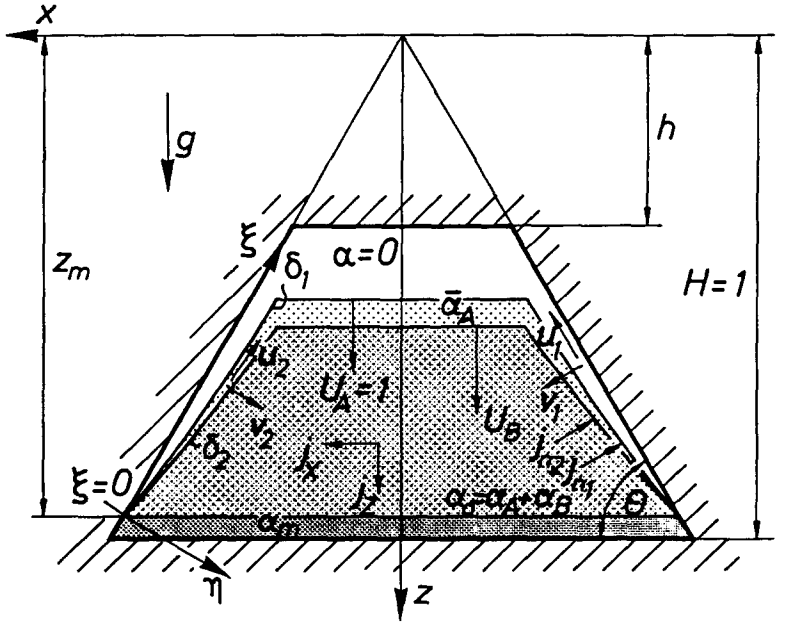

Figure 2. Definition of variables.

between the drift-flux $\mathbf{j}_{sf}$ and the concentration α, that is formally written as

$$\mathbf{j}_{sf} = f(\alpha)\mathbf{e}. \tag{7}$$

The function $f(\alpha)$ is to be determined from suspension mechanics or by experiments. Often an empirical correlation of the power-law form

$$f(\alpha) = \alpha(1 - \alpha)^n, \ (n = \text{const.}) \tag{8}$$

is used. According to Richardson & Zaki (1954), cf. also Wallis (1969, p. 178), the value $n = 4.7$ provides good results for small particle Reynolds numbers.

The existence of a particle-free boundary layer implies the following boundary condition for the normal component j_n of the total volume flux j at the inclined wall (Schneider 1982):

$$\alpha j_n + f(\alpha) \cos\theta = 0, \tag{9}$$

where θ denotes the inclination angle between the horizontal x-axis and the wall (figure 2).

In boundary-layer coordinates (ξ, η) Schneider (1982) derived for a plane wall, a monodispersed suspension and a sedimentation process of type I ($\alpha = \alpha_0 = \text{const}$, classification according to Wallis, 1969, pp. 191–194), a similarity solution of the inviscid boundary-layer flow of the clear liquid:

$$\left.\begin{aligned} \tilde{\psi} &= \tilde{\xi}\left[(2\sin\theta)^{1/2}\lambda - \frac{\alpha_0 \tan\theta}{2f(\alpha_0)}\lambda^2\right], \\ \lambda &= \tilde{\eta}\tilde{\xi}^{1/2}, \end{aligned}\right\} \tag{10}$$

$$\tilde{\delta} = \frac{(2\sin\theta)^{1/2}}{\tan\theta} \cdot \frac{f(\alpha_0)}{\alpha_0}\tilde{\xi}^{1/2}. \tag{11}$$

The stretched tangential velocity $\tilde{u} = u\mathrm{Re}/\mathrm{Gr}$ and the normal velocity $\tilde{v} = v$ are given by the partial derivatives of the stream function $\tilde{\psi}$:

$$\left.\begin{aligned} \tilde{u} &= \frac{\partial\tilde{\psi}}{\partial\tilde{\eta}}, \\ \tilde{v} &= \frac{\partial\tilde{\psi}}{\partial\tilde{\xi}}. \end{aligned}\right\} \tag{12}$$

While the coordinate $\tilde{\xi} = \xi$ remains unchanged, the coordinate $\tilde{\eta} = \eta \cdot \mathrm{Gr}^{1/2}/\mathrm{Re}$. Therefore, [11] for the interface between the suspension and the clear liquid is also stretched with $\mathrm{Gr}^{1/2}/\mathrm{Re}$.

3. BOUNDARY LAYER FLOW OF A MIXTURE HAVING TWO SIZES OF PARTICLES

For the theoretical analysis we assume a mixture with particles of size A and particles of size B that are by definition the larger ones. The deviations of the particles diameter of size B from size A should be small. The volume concentration α_A of size A should be of the same order of magnitude as the volume fraction α_B of size B. The sedimentation process is of type I with a two-dimensional flow field in a roof-shaped, symmetrical vessel. All assumptions are in conformity with our experimental conditions (Schaflinger 1985) (figure 3).

According to [9] we obtain for a suspension with two different particle sizes for the normal component j_{n_1} of the total volume flux at the interface 1 between clear liquid and

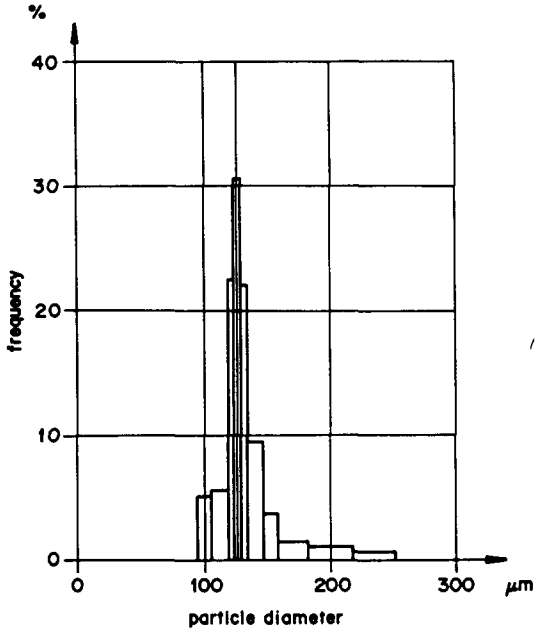

Figure 3. Particle size distribution.

particles with size A

$$j_{n_1} = -\frac{f(\bar{\alpha}_A)}{\bar{\alpha}_A}\cos\theta, \qquad [13a]$$

where $\bar{\alpha}_A$ is the volume concentration within the particle sub-layer.

At the interface 2 between the layer of particles with size A and the suspension with the initial concentration α_0 we obtain the corresponding result for the normal component j_{n_2} of the total flux

$$j_{n_2} = -\frac{f(\alpha_0)}{\alpha_0}(1 + \epsilon)\cos\theta, \qquad [13b]$$

where ϵ is defined as

$$\epsilon = \frac{U_B - U_A}{U_A}. \qquad [14]$$

In the following text the subscript 1 refers to the clear liquid layer and the interface between clear liquid and particles with size A. Subscript 2 refers to the particle sublayer and the interface between the sublayer and the suspension.

Continuity of the total flux density across the interface 2 results in an equation for the unknown concentration $\bar{\alpha}_A$ within the particle sublayer

$$1 + \epsilon\left[1 - \frac{\alpha_A}{\bar{\alpha}_A(1 - \alpha_0)}\right] - \frac{f(\bar{\alpha}_A)\alpha_0}{f(\alpha_0)\bar{\alpha}_A} = 0, \qquad [15]$$

which has to be evaluated numerically. For small values of α_A there is an analytical solution found for the concentration $\bar{\alpha}_A$:

$$\bar{\alpha}_A^2 + \frac{\bar{\alpha}_A}{n}\left[\frac{f(\alpha_0)}{\alpha_0}(1+\epsilon) - 1\right] - \frac{\epsilon\alpha_A}{n}\frac{f(\alpha_0)}{\alpha_0(1-\alpha_0)} = 0 \qquad [16]$$

where n is the exponent according to [8].

Equation [15] was also derived by Smith (1966) when he investigated the horizontal concentration jump appearing in sedimentation of particles with different sizes.

It is an interesting fact following from [15] or [16] that for the limiting case $\epsilon \to 0$: $\bar{\alpha}_A = O(\alpha_0)$ and is independent on the initial concentration α_A of the particle size A. Only when $\alpha_0 \to 0$ and $\epsilon > \alpha_0/f(\alpha_0) - 1$ the concentration within the particle sublayer $\bar{\alpha}_A = O(\alpha_A)$. Figure 4 shows the initial concentration α_A versus the concentration $\bar{\alpha}_A$ within the sublayer for various values of ϵ and with a constant total concentration $\alpha_0 = 0.014$ that was used in our experiments.

From [13] we conclude that the variation of the total volume flux v_2 normal to the wall within the particle sub-boundary-layer has to be of magnitude $(j_{n_1} - j_{n_2})$. Thus, we define a parameter

$$\kappa = \epsilon\frac{\alpha_A}{\bar{\alpha}_A(1-\alpha_0)} \cdot \frac{\rho_f}{\rho\bar{\alpha}_A} \qquad [17]$$

for the magnitude of this difference. $\rho_{\bar{\alpha}_A}$ denotes the density of a suspension with particles A and a concentration of $\bar{\alpha}_A$.

It can be shown that the particle sub-boundary-layer requires the following stretched variables:

$$\left.\begin{aligned} \tilde{u}_2 &= \mathrm{ReGr}^{-1/2}\kappa^{-1/2}\mu_2, \\ \tilde{v}_2 &= \kappa^{-1}(v_2 - j_{n_2}), \\ \tilde{\eta}_2 &= \mathrm{Gr}^{1/2}\,\mathrm{Re}^{-1}\kappa^{-1/2}(\eta - \delta_1), \\ \tilde{\xi}_2 &= \xi, \end{aligned}\right\} \qquad [18]$$

with $\delta_1 = \delta \cdot \mathrm{Re} \cdot \mathrm{Gr}^{-1/2}$; δ is given by [11], where α_0 has to be replaced by $\bar{\alpha}_A$.

Taking [13] into account, the equation of motion in tangential direction becomes

$$j_n\frac{\partial\tilde{u}_2}{\partial\tilde{\eta}_2} = \frac{\rho_f}{\rho_{\bar{\alpha}_A}}\frac{\bar{\alpha}_B}{\alpha_0}\sin\theta + \mathrm{Gr}^{1/2}\,\mathrm{Re}^{-2}\,\kappa^{-1/2}\frac{\nu_{\bar{\alpha}_A}}{\nu_f}\frac{\partial^2\tilde{u}_2}{\partial\tilde{\eta}_2^2}, \qquad [19]$$

where $\bar{\alpha}_B = \alpha_0 - \bar{\alpha}_A$.

ν_{α_A} is the kinematic viscosity of the suspension containing particles A with a concentration $\bar{\alpha}_A$. ν_{α_0} is the kinematic viscosity of the suspension with the total concentration α_0. It is related to the dynamic viscosity μ_α of the suspension by $\nu_\alpha = \mu_\alpha/\rho_\alpha$ with $\rho_\alpha = (1-\alpha)\rho_f + \alpha\rho_s$.

The relevance of the viscous term of [19] depends on the magnitude of the thickness ratio of the particle sub-boundary-layer to the free shear layer $\delta_2/\delta_f = O(\mathrm{Re}^2\mathrm{Gr}^{-1/2}\kappa^{1/2})$. Additionally a complete analysis has to make sure that matching can be accomplished with u_1, the velocity in the clear liquid layer, and u_2, the velocity in the particle sub-boundary-layer as well as with u_2, and u, the velocity within the bulk. The thickness of the free shear layer has to be $\delta_f = O(\mathrm{Re}^{-1})$. Hence it follows that the tangential velocity u_f is as large as $\mathrm{Gr}/\mathrm{Re}^3$. In this manner, the dimensionless group $\mathrm{Gr}/\mathrm{Re}^3$ determines the relative thickness of the sublayer and its structure.

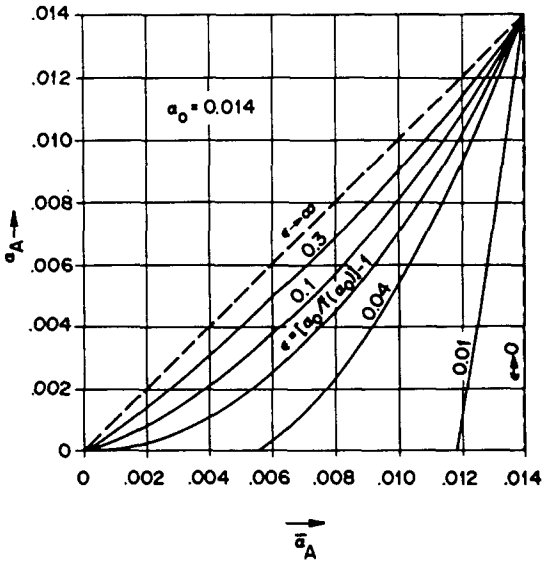

Figure 4. Volume fraction solids of size A within the bulk of the suspension (α_A) versus the volume fraction of size A within the particle sub-boundary layer ($\bar{\alpha}_A$).

a) $Gr/Re^3 \to 0$: An inviscid part of the particle sub-boundary layer exists, when $\delta_2/\delta_f \to \infty$

b) $Gr/Re^3 = O(1)$: From $\delta_2 = O(\delta_f)$ it follows that the particle sub-boundary-layer is no longer inviscid

c) $Gr/Re^3 \to \infty$: The particle sub-boundary-layer lies entirely within the viscous free shear layer whereby $\delta_2/\delta_f \to 0$

Because the last case (c) excludes the experimentally observed effects (Schaflinger 1985), a more detailed analysis for this case will not be given. The other two cases (a, b) will be investigated in detail.

3.1 *Sub-boundary layer with* $Gr/Re^3 \to 0$

3.1.1 *The inviscid part of the sub-boundary-layer.* On the one hand, analysing this case requires both Gr/Re^3 and Gr/Re^4 to be small. On the other hand, the assumption $\kappa^{1/2} Re^2 Gr^{-1/2} \to \infty$ has to be satisfied and we derive the following restrictions for κ

$$1 \gg \kappa \gg Gr/Re^4. \tag{20}$$

The equation of motion, the continuity equation and the appropriate boundary conditions are given as follows:

$$\frac{\partial \tilde{u}_2}{\partial \tilde{\eta}_2} = -\frac{\rho_f \bar{\alpha}_B}{\rho_{\bar{\alpha}_A} f(\alpha_0)} \tan\theta, \tag{21}$$

$$\frac{\partial \tilde{u}_2}{\partial \tilde{\xi}_2} + \frac{\partial \tilde{v}_2}{\partial \tilde{\eta}_2} = 0, \tag{22}$$

$$\tilde{u}_2 = 0 \quad \text{at} \quad \tilde{\eta}_2 = \tilde{\delta}_2, \tag{23a}$$

$$\tilde{v}_2 = 0 \quad \text{at} \quad \tilde{\eta}_2 = \tilde{\delta}_2, \tag{23b}$$

$$\tilde{v}_2 = \frac{f(\alpha_0)\rho_{\bar{\alpha}_A}}{\alpha_0 \rho_f} \cos\theta \quad \text{at} \quad \tilde{\eta}_2 = 0. \tag{23c}$$

The boundary condition [23a] is only correct, when $\mathrm{Gr}^{1/2}\,\mathrm{Re}^{-1}\,\kappa^{1/2} \to \infty$, otherwise $\mu_2 = O[j_t(\xi)]$ where j_t is the tangential component of the total volume flux density and given by Schneider (1982). When $\alpha_0 \to 0$

$$j_t = \frac{1}{\sin\theta - \xi \sin^2\theta} - \sin\theta. \tag{24}$$

Defining a streamfunction $\tilde{\psi}_2$, analogous to [12], we obtain the solution of [21] ÷ [23]

$$\tilde{\psi}_2 = \left(2\frac{\bar{\alpha}_B}{\alpha_0}\sin\theta\right)^{1/2}\tilde{\xi}_2^{1/2}\,\tilde{\eta}_2 - \frac{\bar{\alpha}_B\tilde{\eta}_2^2\tan\theta}{2f(\alpha_0)}\cdot\frac{\rho_f}{\rho_{\bar{\alpha}_A}} - \tilde{\xi}_2\frac{f(\alpha_0)\rho_{\bar{\alpha}_A}}{\alpha_0\rho_f}\cos\theta. \tag{25}$$

The thickness of a particle sub-boundary layer is found from [25] with [12] and [23a]

$$\tilde{\delta}_2 = \frac{f(\alpha_0)}{(\bar{\alpha}_B\alpha_0)^{1/2}}\frac{(2\sin\theta)^{1/2}}{\tan\theta}\frac{\rho_{\bar{\alpha}_A}}{\rho_f}\tilde{\xi}_2^{1/2}. \tag{26}$$

The inviscid boundary layer flow cannot satisfy the condition of continuous shear stress at the interface 1 and at the interface 2, respectively. Hence free shear layers at both interfaces have to be introduced.

3.1.2 *The free shear layers at the interfaces 1 and 2.* Matching the inviscid particle sublayer at the interface 1 with the clear liquid layer, as well as at the interface 2 with the bulk requires the following stretched variables:

$$\left.\begin{aligned}
\tilde{u}_{F_{1,2}} &= \mathrm{Re}^3\,\mathrm{Gr}^{-1}[u_{F_{1,2}} - \sigma u_2 + (\sigma - 1)j_t(\xi)]\\
\tilde{v}_{F_{1,2}} &= \mathrm{Re}\,(\mathrm{Gr}\,\kappa)^{-\sigma/2}(v_{F_{1,2}} - j_{n_{1,2}}),\\
\tilde{\eta}_{F_{1,2}} &= \mathrm{Re}\,[\eta - (\delta_1 + \delta_2) + \sigma\delta_2],\\
\tilde{\xi}_{F_{1,2}} &= \xi,
\end{aligned}\right\} \tag{27}$$

whereby at the interface 1: $\sigma = 1$, and at the interface 2: $\sigma = 0$.

In terms of the stretched variables according to [27], the momentum and continuity equations become:

$$\left.\begin{aligned}
\tilde{\eta}_{F_{1,2}} < 0\text{:}\; & j_{n_{1,2}}\left(\frac{\partial\tilde{u}_{F_{1,2}}}{\partial\tilde{\eta}_{F_{1,2}}} + \sigma\frac{\bar{\alpha}_B}{\alpha_0}\frac{\sin\theta}{j_{n_{1,2}}}\right) = \left(\frac{\bar{\alpha}_B}{\alpha_0}\frac{\rho_f}{\rho_{\bar{\alpha}_A}}\right)^{1-\sigma}\sin\theta + \left(\frac{\nu_{\bar{\alpha}_A}}{\nu_f}\right)^{1-\sigma}\frac{\partial^2\tilde{u}_{F_{1,2}}}{\partial\tilde{\eta}_{F_{1,2}}^2},\\
\tilde{\eta}_{F_{1,2}} > 0\text{:}\; & j_{n_{1,2}}\frac{\partial\tilde{u}_{F_{1,2}}}{\partial\eta_{F_{1,2}}} = \frac{\nu_{\bar{\alpha}_{A,0}}}{\nu_f}\frac{\partial^2\tilde{u}_{F_{1,2}}}{\partial\tilde{\eta}_{F_{1,2}}^2},
\end{aligned}\right\} \tag{28}$$

$$\tilde{\eta}_{F_{1,2}} \lesseqgtr 0\text{:}\; \sigma\frac{\partial\tilde{u}_2}{\partial\tilde{\xi}_2} + (\sigma - 1)\frac{\partial j_t}{\partial\tilde{\xi}_{F_2}} + \frac{\partial\tilde{v}_{F_{1,2}}}{\partial\tilde{\eta}_{F_{1,2}}} = 0 \tag{29}$$

The matching conditions are:

$$\lim_{\tilde{\eta}_{F_{1,2}}\to+\infty}\tilde{u}_{F_{1,2}} = 0, \tag{30a}$$

$$\lim_{\tilde{\eta}_{F_{1,2}}\to-\infty}\frac{\partial\tilde{u}_{F_{1,2}}}{\partial\tilde{\eta}_{F_{1,2}}} = (1 - 2\sigma)\frac{\sin\theta}{j_{n_{1,2}}}\left[\frac{\bar{\alpha}_B}{\alpha_0}\left(\frac{\rho_f}{\rho_{\bar{\alpha}_A}}\right)^{1-\sigma} - \sigma\right]. \tag{30b}$$

The total volume flux and the shear stress have to be continuous at the interfaces (1, 2). This yields the boundary conditions:

$$\left.\begin{aligned} \lim_{\tilde{\eta}_{F_{1,2}}\to 0^-}\left(\nu_{f,\bar{\alpha}_A}\rho_{f,\alpha_A}\frac{\partial\tilde{u}_{F_{1,2}}}{\partial\tilde{\eta}_{F_{1,2}}}\right) &= \lim_{\tilde{\eta}_{F_{1,2}}\to 0^+}\left(\nu_{\bar{\alpha}_{A,0}}\rho_{\bar{\alpha}_{A,0}}\frac{\partial\tilde{u}_{F_{1,2}}}{\partial\tilde{\eta}_{F_{1,2}}}\right)\\ \lim_{\tilde{\eta}_{F_{1,2}}\to 0^-}\tilde{u}_{F_{1,2}} &= \lim_{\tilde{\eta}_{F_{1,2}}\to 0^+}\tilde{u}_{F_{1,2}}\\ \lim_{\tilde{\eta}_{F_{1,2}}\to 0^-}\tilde{v}_{F_{1,2}} &= \lim_{\tilde{\eta}_{F_{1,2}}\to 0^+}\tilde{v}_{F_{1,2}} \end{aligned}\right\} \quad [31]$$

The solution of [28] satisfying to the auxiliary conditions [30] and [31] is found to be

$$\left.\begin{aligned} \tilde{\eta}_{F_{1,2}} < 0\text{: } \tilde{u}_{F_{1,2}} &= \left(\tilde{\eta}_{F_{1,2}} + \frac{\rho_{f,\bar{\alpha}_A}}{\rho_{\bar{\alpha}_{A,0}}}j_{n_{1,2}}^{-1}\right)\left[\frac{\bar{\alpha}_B}{\alpha_0}\left(\frac{\rho_f}{\rho_{\bar{\alpha}_A}}\right)^{1-\sigma} - \sigma\right](1-2\sigma)\frac{\sin\theta}{j_{n_{1,2}}}\\ \tilde{\eta}_{F_{1,2}} > 0\text{: } \tilde{u}_{F_{1,2}} &= \left[\frac{\alpha_B}{\alpha_0}\left(\frac{\rho_f}{\rho_{\bar{\alpha}_A}}\right)^{1-\sigma} - \sigma\right](1-2\sigma)\\ &\quad\cdot\frac{\rho_{f,\bar{\alpha}_A}}{\rho_{\bar{\alpha}_{A,0}}}\left(\frac{\nu_{\bar{\alpha}_A}}{\nu_f}\right)^{1-\sigma}\frac{\sin\theta}{j_{n_{1,2}}^2}\cdot\exp\left(\frac{\nu_f}{\nu_{\bar{\alpha}_{A,0}}}j_{n_{1,2}}\tilde{\eta}_{F_{1,2}}\right). \end{aligned}\right\} \quad [32]$$

The limiting case $\epsilon \to 0$, especially when a monodispersed suspension is considered, leads to $\delta_2 = 0$. Thus $\tilde{u}_{F_2} \to \tilde{u}_F$, the tangential velocity within the free shear layer introduced by Schneider (1982). However, the stretched variables distinguished by Schneider concerning $\mathrm{Gr/Re^3} = \mathrm{O}(1)$ or $\mathrm{Gr/Re^3} \to 0$ are incorrect, because matching fails in the case $\mathrm{Gr/Re^3} \to 0$. The correct stretched variables are given by [27] with $\sigma = 0$.

3.2 *Sub-boundary layer with* $Gr/Re^3 = O(1)$

This case requires that the thickness of the particle sub-boundary layer $\delta_2 = \mathrm{O}(\delta_F)$. Hence the parameter

$$\kappa = \mathrm{O(Gr/Re^4)} = \mathrm{O(Re^2/Gr)} = \mathrm{O(Re^{-1})}, \quad [33]$$

and the appropriate stretching transformations are

$$\left.\begin{aligned} \tilde{u} &= u,\\ \tilde{v} &= \mathrm{Re}\,(v_2 - j_{n_2}),\\ \tilde{\eta} &= \mathrm{Re}\,(\eta_2 - \delta_1),\\ \tilde{\xi} &= \xi_2. \end{aligned}\right\} \quad [34]$$

Taking [34] into account we derive the momentum equation for the particle sub-boundary layer from [19]

$$\tilde{\eta} = \tilde{\eta}_2 > 0\text{: } j_{n_2}\frac{\partial\tilde{u}_2}{\partial\tilde{\eta}_2} = \frac{\bar{\alpha}_B}{\alpha_0}\frac{\rho_f}{\rho_{\bar{\alpha}_A}}\sin\theta + \frac{\nu_{\bar{\alpha}_A}}{\nu_f}\frac{\partial^2\tilde{u}_2}{\partial\tilde{\eta}_2^2}, \quad [35]$$

with the condition for the interface B

$$\tilde{v}_2 = 0 \qquad \text{at} \qquad \tilde{\eta}_2 = \tilde{\delta}_2. \quad [36]$$

The equation of continuity [22] remains unchanged.

In stretched variables defined by [34], the equation of motion for the free shear layer at the interface 1, and the free shear layer at the interface 2 becomes

$$j_{n_2} \frac{\partial \tilde{u}_{F_{1,2}}}{\partial \tilde{\eta}_{F_{1,2}}} = \sigma \sin\theta + \left(\frac{\nu_{\alpha_0}}{\nu_f}\right)^{1-\sigma} \frac{\partial^2 \tilde{u}_{F_{1,2}}}{\partial \tilde{\eta}^2_{F_{1,2}}}, \tag{37}$$

whereby $\sigma = 1$ for $\tilde{\eta} = \tilde{\eta}_{F_1}$, and $\sigma = 0$ for $\tilde{\eta} = \tilde{\eta}_{F_2}$.

The continuity equation [22] is used again with subscript F_1 or F_2 replacing subscript 2.

The matching conditions are found to be

$$\lim_{\tilde{\eta}_{F_1} \to -\infty} \frac{\partial \tilde{u}_{F_1}}{\partial \tilde{\eta}_{F_1}} = \frac{\sin\theta}{j_{n_2}}, \tag{38a}$$

$$\lim_{\tilde{\eta}_{F_2} \to +\infty} \tilde{u}_{F_2} = j_t(\xi), \tag{38b}$$

while the appropriate boundary conditions become

$$\left.\begin{aligned} \lim_{\tilde{\eta}_2 \to \tilde{\delta}^-} \left(\nu_{\bar{\alpha}_A} \rho_{\bar{\alpha}_A} \frac{\partial \tilde{u}_2}{\partial \tilde{\eta}_2}\right) &= \lim_{\tilde{\eta}_2 \to \tilde{\delta}^+} \left(\nu_{\alpha_0} \rho_{\alpha_0} \frac{\partial \tilde{u}_{F_2}}{\partial \tilde{\eta}_{F_2}}\right), \\ \lim_{\tilde{\eta}_2 \to \tilde{\delta}^-} \tilde{u}_2 &= \lim_{\tilde{\eta}_2 \to \tilde{\delta}^+} \tilde{u}_{F_2}, \\ \lim_{\tilde{\eta}_2 \to \tilde{\delta}^-} \tilde{v}_2 &= \lim_{\tilde{\eta}_2 \to \tilde{\delta}^+} \tilde{v}_{F_2} \end{aligned}\right\} \tag{39}$$

and

$$\left.\begin{aligned} \lim_{\tilde{\eta}_{F_1} \to 0^-} \left(\nu_F \rho_f \frac{\partial \tilde{u}_{F_1}}{\partial \tilde{\eta}_{F_1}}\right) &= \lim_{\tilde{\eta}_{F_1} \to 0^+} \left(\nu_{\bar{\alpha}_A} \rho_{\bar{\alpha}_A} \frac{\partial \tilde{u}_2}{\partial \tilde{\eta}_2}\right), \\ \lim_{\tilde{\eta}_{F_1} \to 0^-} \tilde{u}_{F_1} &= \lim_{\tilde{\eta}_{F_1} \to 0^+} \tilde{u}_2 \\ \lim_{\tilde{\eta}_{F_1} \to 0^-} \tilde{v}_{F_1} &= \lim_{\tilde{\eta}_{F_1} \to 0^+} \tilde{v}_2 = \widetilde{\mathrm{Re}}, \end{aligned}\right\} \tag{40}$$

with $\widetilde{\mathrm{Re}} = \mathrm{Re} f(\alpha_0) \rho_{\alpha A} \kappa \cos\theta / \alpha_0 \rho_f$.

Taking [24] into account, the solution of [35]–[40] in the case $\alpha_0 \to 0$ is found to be

$$\tilde{u}_{F_1} = \frac{\tan\theta - \sin\theta - A}{\cos\theta} + C_1(\tilde{\xi}_2), \tag{41a}$$

$$\tilde{u}_2 = \frac{\tan\theta - A}{\cos\theta} \exp(-\tilde{\eta}_2 \cos\theta) - \tilde{\eta}_2 A + C_1(\tilde{\xi}_2), \tag{41b}$$

$$\tilde{u}_{F_2} = C_2(\tilde{\xi}_2) \exp(-\tilde{\eta}_{F_2} \cos\theta) + j_t(\tilde{\xi}_2), \tag{41c}$$

$$\tilde{v}_2 = \widetilde{\mathrm{Re}} - C_1'(\tilde{\xi}_2)\tilde{\eta}_2, \tag{41d}$$

$$\tilde{\delta}_2 = \widetilde{\mathrm{Re}} / C_1'(\tilde{\xi}_2), \tag{41e}$$

$$C_1' = A \widetilde{\mathrm{Re}} / (C_1 + B), \tag{41f}$$

$$C_2 = \frac{\tan\theta - A}{\cos\theta} + A \exp(\tilde{\delta}_2 \cos\theta), \tag{41g}$$

$$B = \sin\theta - \frac{A}{\cos\theta} - \frac{1}{\sin\theta - \xi_2 \sin^2\theta}, \qquad [41h]$$

$$A = \frac{\alpha_B}{\alpha_0} \tan\theta. \qquad [41i]$$

In the limiting case $\tilde{\xi}_2 \to 0$ integrating [41f] leads to the analytical solution

$$C_1 = D + (2\,\widetilde{\mathrm{Re}}\,\tilde{\xi}_2 A)^{1/2}, \qquad [42]$$

so that the equation for the interface B becomes

$$\delta_2 = (C_1 + B)/A. \qquad [43]$$

Figure 5 shows the particle sub-boundary layer for two different values of κ compared to the clear liquid layer. The initial concentration α_0 as well as the vessel's geometry are taken from our experiments (Schaflinger 1985). Under these conditions settling in clear water yields $\mathrm{Gr}/\mathrm{Re}^3 = 0.07$ and $\mathrm{Gr}/\mathrm{Re}^4 = 0.05$. The measured particle size distribution (figure 3) justifies the assumption that α_A is within the range of 0.006 and $\kappa \sim 0.1$. In this case an inviscid particle sub-boundary layer appears with a relatively large velocity upwards. The theoretical prediction [26] complies well with the experimental observations (figure 5). When $\kappa = 0.05$ the particle sublayer is governed by the solution according to [41], and is no longer inviscid (dashed line in figure 5).

4. CONCLUSIONS

A theory by Schneider (1982), which is valid for small values of $\mathrm{Re}^2/\mathrm{Gr}$ and large values of $\mathrm{Re}^4/\mathrm{Gr}$, deals with batch sedimentation of a monodispersed suspension in a symmetrical, roof-shaped vessel. Experiments show some puzzling effects that are not predicted by this theory, e.g. a particle sub-boundary layer between the clear liquid layer at the inclined wall and the bulk of the suspension. Particles are moving upward within that sublayer with a relatively high velocity. This particle stream propagates into the clear liquid above the suspension, where it is observed as protruding "horn" deforming the initially horizontal interface. Subsequently this effect gives rise to an oscillation of the interface. In order to explain these effects the abovementioned theory is enhanced by taking into account

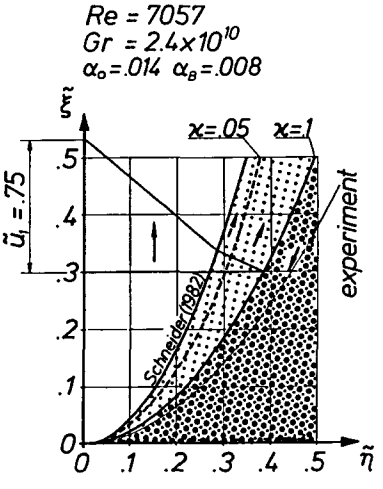

Figure 5. Boundary layer for two sizes of particles and comparison with the experiment.

nonuniform particle sizes. In conformity with our experimental conditions (Schaflinger 1985), small deviations of one particle size A from the other size B are taken as a basis for a theoretical analysis. Thereby it is shown that the particle sub-boundary layer is influenced by the deviations of particle size, as well as by the ratio of the partial volume fractions. In the case of two different particle sizes within the suspension the concentration of solids within the particle sub-boundary layer is of the same magnitude as the total bulk-concentration if the deviations of the nominal size are small.

The structure of the particle sub-boundary layer depends on the magnitude of Gr/Re^3. When $Gr/Re^3 \to 0$ the sublayer is mainly inviscid. To satisfy the condition of continuous shear stress at both interfaces, free shear layers have to be introduced.

The results show that in the case of nonuniform particle size within a suspension there exists an upstreaming particle sub-boundary layer. This particle stream explains the observed phenomena like protruding "horns," resuspending of particles and a subsequent oscillation of the interface suspension-purified liquid. The calculated particle sub-boundary layer thickness is in fair agreement with the experimental data.

In the case of large deviations of one particle size from the other, and a very small volumetric concentration of one size compared with the total concentration, the observed effects cannot be explained. A particle sub-boundary layer does exist, but the volume fraction of solids within this layer is too small in comparison with the experiments. For more details cf. the Appendix.

Acknowledgements—This work is an abridged version of the theoretical section of the author's PhD thesis. The author should like to thank Professor Dr. W. Schneider for supervising this work and for many helpful comments.

REFERENCES

ACRIVOS, A. & HERBOLZHEIMER, E. 1979 Enhanced sedimentation in settling tanks with inclined walls. *J. Fluid Mech.* **92,** 435–457.

AMBERG, G., DAHLKILD, A. A., BARK, F. H. & HENNINGSON, D. S. 1984 On time-dependent settling of a dilute suspension in a rotating conical channel. Submitted to *J. Fluid Mech.*

ANESTIS, G. & SCHNEIDER, W. 1983 Application of the theory of kinematic waves to the centrifugation of suspensions. *Ing. Archiv.* **53,** 399–407.

DAVIS, R. H., HERBOLZHEIMER, E. & ACRIVOS, A. 1982 The sedimentation of polydisperse suspensions in vessels having inclined walls. *Int. J. Multiphase Flow* **8,** 571–585.

GREENSPAN, H. P. & UNGARISH, M. 1982 On hindered settling of particles of different sizes. *Int. J. Multiphase Flow* **8,** 587–604.

HERBOLZHEIMER, E. 1983 Stability of the flow during sedimentation in inclined channels. *Phys. Fluids* **26,** 2043–2054.

HERBOLZHEIMER, E. & ACRIVOS, A. 1981 Enhanced sedimentation in narrow tilted channels. *J. Fluid Mech.* **108,** 485–499.

HILL, W. D., ROTHFUS, R. R. & LI, K. 1977 Boundary enhanced sedimentation due to settling convection. *Int. J. Multiphase Flow* **3,** 561–583.

KINOSITA, K. 1949 Sedimentation in tilted vessels. *J. Colloid. Interface Sci.* **4,** 525–536.

LEUNG, W. F. & PROBSTEIN, R. F. 1983 *J and EC Process Design and Development* **22,** 58.

NAKAMURA, H. & KURODA, K. 1937 La cause de l'accélération de la vitesse de sédimentation des suspensions dans les récipients inclinés. *Keijo J. Med.* **8,** 256–296.

PONDER, E. 1925 On sedimentation and rouleaux formation. *Quart. J. Exp. Physical.* **15,** 235–252.

RICHARDSON, J. F. & ZAKI, W. N. 1954 Sedimentation and fluidization: Part I. *Trans. Inst. Chem. Engrs.* **32,** 35–53.

SCHAFLINGER, U. 1985 Experiments on sedimentation beneath downward-facing inclined walls. *Int. J. Multiphase Flow* **11**, 189–199.

SMITH, T. N. 1966 The sedimentation of particles having a dispersion of sizes. *Trans. Inst. Chem. Engrs.* **44**, T153–T157.

SCHNEIDER, W. 1982 Kinematic-wave theory of sedimentation beneath inclined walls. *J. Fluid Mech.* **120**, 323–346.

SCHNEIDER, W., ANESTIS, G. & SCHAFLINGER, U. 1985 Sediment composition due to settling of particles of different sizes. *Int. J. Multiphase Flow* **11**, 419–423.

WALLIS, G. B. 1969 *One-dimensional Two-phase Flow.* McGraw-Hill, New York.

ZAHAVI, E. & RUBIN, E. 1975 Settling of solid suspensions under and between inclined surfaces. *Ind. Eng. Chem., Process Des. Develop.* **14**, 34–40.

APPENDIX: SUB-BOUNDARY LAYER IN THE CASE OF LARGE DEVIATIONS OF ONE PARTICLE SIZE FROM THE OTHER

Consider the case of large deviations of one particle size from the other. The volumetric concentration of one particle size is assumed to be very small in comparison with the total volume fraction of solids ($\alpha = \alpha_A + \alpha_B$). Subscript A refers to particles with the smaller size. Both particle Reynolds numbers are assumed to be small, in order that Stoke's law [3] remains valid. Thus, the structure of the flow field, both the bulk and the boundary layer, is given by the results for a monodispersed suspension. A linear superposition of Schneider's solution for the streamfunction ψ_f for the liquid as a result of [4]–[9], as well as the boundary conditions given by the vessel's geometry; and the settling velocity of a single nonuniform particle within the whole swarm of solids with concentration α_0 yields the following particle stream function for the deviating species:

$$\psi_{s_a} = x\frac{f(\alpha_0)}{\alpha_0}\left[(1+\epsilon)^{1-k/2}\cdot\frac{z_m}{z}+\frac{\epsilon}{(1-\alpha_0)}k\right]. \qquad [A1]$$

z_m the position of the kinematic shock separating the sediment from the suspension, is given by

$$z_m = 1 - \frac{f(\alpha_0)}{\alpha_m - \alpha_0}, \qquad [A2]$$

where α_m denotes the concentration of the sediment which is at rest. The parameter k is defined to be $+1$ if the main species are smaller than the deviating ones. If the main particles are greater than the deviating particles, $k = -1$.

Equation [A1] shows that the particle paths are located between straight lines parallel to the vertical axis ($k = 1, \epsilon \to \infty$) and the liquid streamlines in the suspension ($k = -1, \epsilon \to \infty$). The case $\epsilon \to 0$ leads to the solution for the particle streamlines calculated by Schneider (1982).

In the case $k = -1$ the deviating particles penetrate the clear liquid boundary layer. Following the same ideas as mentioned above, we obtain by a linear superposition the equation for the particle paths within the layer 2

$$\tilde{\psi}_{s_2} = (1+\epsilon)\left[(2\sin\theta)^{1/2}\tilde{\xi}^{1/2}\tilde{\eta} - \frac{\tilde{\eta}^2\alpha_0\tan\theta}{2f(\alpha_0)}\right] - \tilde{\xi}\cos\theta - \tilde{\eta}\sin\theta. \qquad [A3]$$

If the main particles are greater than the deviating ones, the penetration depth within the boundary layer is given by the location where the component of the particle velocity normal to the wall vanishes. This leads to the equation for the interface between the liquid that

remains particle-free and the liquid layer with penetrated solids:

$$\tilde{\delta}_1 = (1 + \epsilon)^{-1} \frac{(2 \sin \theta)^{1/2}}{\tan \theta} \tilde{\xi}^{1/2}. \qquad [A4]$$

For small values of $\epsilon \leq \alpha_0/f(\alpha_0) - 1$ $(k = -1)$ an evaluation of [A3], [A4] for an upstreaming particle sub-boundary layer fails, because the particle concentration within the layer is greater than the volume fraction of the deviating solids within the bulk (figure 4) and must be determined from the total flux continuity across the interface 2. Thereby the sub-boundary layer is influenced by the particles, too.